Metallurgical Coating to Reduce Graphite Degeneration at the Surface Zone of Compacted Graphite Iron Castings

U. C. Nwaogu[a] and W. Stets[b].

Foundry R&D Centre,

Foseco Nederland BV,

Pantheon 30, 7521 PR Enschede,

The Netherlands.

[a]Ugo.Nwaogu@foseco.com and [b]Wolfram.Stets@foseco.com

International Symposium on the Science and Processing of Cast Iron (SPCI-XI), 2017
Jönköping, Sweden

Abstract

The irreversible trend towards higher peak firing pressures have prompted engine designers to seek stronger materials in order to meet their durability targets without increasing the size or weight of their engines. Therefore, with at least 75% increase in ultimate tensile strength, 35-40% increase in elastic modulus and approximately double of the fatigue strength of grey cast iron, compacted graphite iron ideally fits to meet the current and future requirements for diesel engines design. Currently, component design is limited by the degeneration of the compacted graphite (CG) in the rim zone of the compacted graphite iron castings. The reduction/elimination of this by using an active coating, will create significant values for the design engineers. This paper highlights the performance of a new FOSECO foundry coating, ACTICOTE CG800, for CGI application to reduce CG degeneration at the rim zone. The ACTICOTE CG800 was specially formulated, produced and characterized according to foundry application specifications. Casting simulations were performed to validate the test models for the coating-casting trials. The ACTICOTE CG800 was benchmarked alongside other commercial coatings for the same application using the customized test model and further on commercial CGI water jackets and cylinder heads, in a foundry known for series production of CGI castings. The investigation of the microstructures at the rim zone of the castings was performed using optical microscope. The results from the trials and investigations show that the ACTICOTE CG800 showed superior performance in the reduction of the CG degeneration at the rim zone of CGI castings.

Key words: Coating, Compacted graphite iron, Compacted graphite degeneration, Flake graphite, Metallurgy, Heating microscopy, Image analysis

1. Introduction

With tightening emission legislation for combustion engines, there is an increasing trend for the wider adoption of Compacted Graphite Iron (CGI) for automotive components, specifically blocks - to enable higher combustion pressures and reduce overall component weight. Currently, component design in CGI is limited by the reversion or degeneration of the compacted graphite (CG), resulting in a layer of flake graphite (FG) in the rim zone of the casting [1, 2]. An example of the microstructure of a CGI casting rim zone with CG degeneration is shown in Fig. 1.

This defect commonly occurs in ductile iron (DI) and compacted graphite iron (CGI) grades of cast iron. The average thickness of the degenerated layer for thin wall DI castings ranged from 0.15 to 0.45 mm, while for CGI it ranged from 0.7 to 2.5 mm [3]. It was reported that a 0.1 to 3.0 mm thick degenerated graphite layer often occurs on ductile iron casting depending on the casting wall thickness and cooling rate [4]. The presence of this degenerated layer of graphite significantly reduces the mechanical properties (fatigue limit, elongation, etc.) of the component in the area where it occurs [2, 5]. Controlling the degeneration of CG at the surface rim zone requires an understanding of the effects of melt chemistry, melt temperature, cooling and solidification rates and the interaction between the metal and the mould/core surface. The assumption is that the direct cause of graphite degeneration, resulting in in a layer of FG as seen in Fig. 1, is the depletion of magnesium (Mg) at the surface layer of the casting. This is due to the reaction of Mg with sulphur and oxygen present in the moulding materials and/or in the mould atmosphere. The reactions are

$$[Mg] + [S] \rightarrow MgS_{(s)} \quad 1.1$$

$$[Mg] + [O] \rightarrow MgO_{(s)} \quad 1.2$$

These processes occur in the vicinity of the mould/core wall.

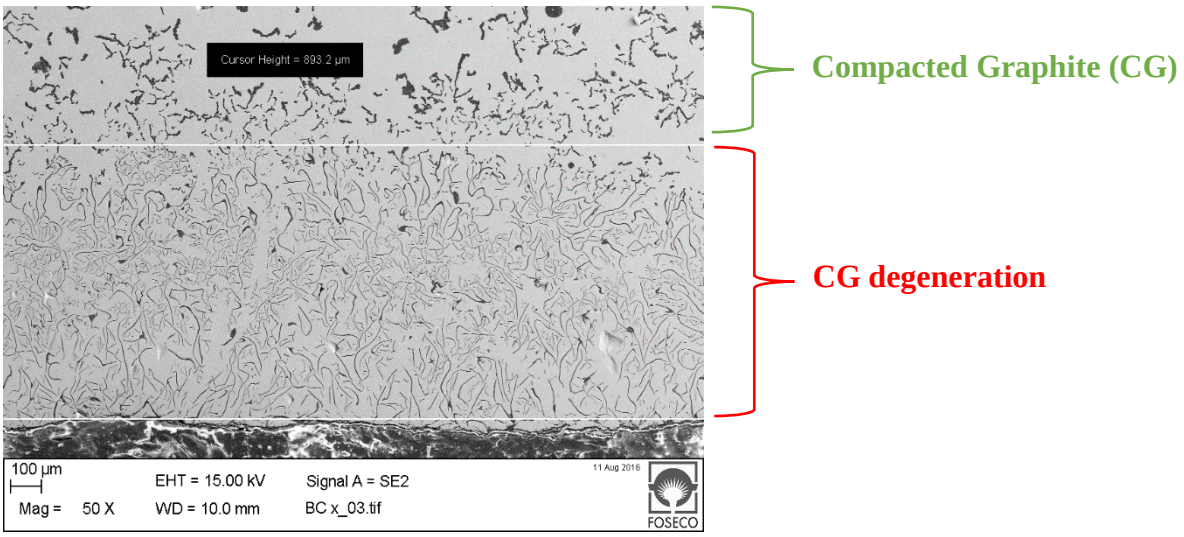

Fig. 1: Compacted graphite reversion layer of flake graphite at the rim zone in a CGI casting

Another mechanism for the formation CG degenerated layer at the rim zone is the influence of solidification kinetics effects (larger undercooling at the interface). Large undercooling at the mould/metal interface favours the precipitation and growth of austenite dendrites that rejects Mg at the solidification front. This leads to low Mg and flake graphite structure at the rim zone close to the metal/mould or core interface with higher nodularity zone further inside the bulk of the castings [2, 6]. According to ISO 16112-2006-08-01, CGI shall have a minimum of 80% of the graphite in vermicular form (form III in accordance with ISO 945), and the remaining 20% of the graphite particles should be of form VI or form V in accordance with ISO 945. Flake (lamellar) graphite (form I and form II according to ISO 945) is not permitted, except within the surface rim zone of the casting [7].

With the mechanisms of formation of degenerated graphite highlighted, its formation reduction may be achieved by reducing the extent of Mg depletion at the interface region and decreasing undercooling at the mould wall. Foundry coatings are generally applied to improve the surface finish of castings and prevent the occurrence of surface defects on castings [8, 9, 10], but do not prevent the occurrence of degeneration of CG to FG. However, it has been reported that

specially formulated foundry coatings have been used to reduce the occurrence of this defect by applying about 0.20 – 0.25 mm dry layer thickness of the coating on the moulds or cores containing 0.02% sulphur [11]. Riposal et al, [4] reported the use of coatings based on desulphurizer (Al_2O_3, $CaCO_3$, Basic slag, CaF_2, Talc), and sinterable materials expected to act as protective layers for the reduction of the occurrence of the defect. Surface layer has been significantly reduced by CaO coatings, due to its reaction with SO_2 and its desulphurization activity. From their findings, they concluded that mold coatings based on the generation of desulphurization agents (such as CaO or MgO) are more effective than protective coatings where the density is a problem. Boonmee and Stefanescu also applied mould coatings as a means of reducing the degeneration of the CG to FG [12]. In their study, they used three types of coatings namely, inactive coatings (mica based, zircon based and boron nitride) – coatings that are completely inert with respect to the melt, active coatings (ferrosilicon and graphite) – coatings that alter the local chemistry of the melt and reactive coatings (CaO, MgO and FeSiMg) – coating that have a chemical reaction with the melt, such as deoxidation and desulphurization. They found out that various coatings have influence on the degeneration of the CG to FG at certain various conditions. They further concluded that the coating made with FeSiMg was the most effective in reducing the degenerated CG layer thickness of iron of eutectic composition at all cooling rates investigated in their work. It was observed by the authors that most of the filler materials used by the above mentioned researchers are not compatible with the universal carrier liquid, water.

The main objective of this paper is to highlight the performance of a newly developed water-based coating, ACTICOTE CG800 (CG800), produced by FOSECO. This coating is used to mitigate the degeneration of the CG to FG, in CGI castings. The performance of this new product is based on the synergistic effect of insulation and optimized permeability provided the coating.

2. Experimental Procedure

The experimental part of this paper is divided into two sections namely Coating Technology and Casting Technology

2.1 Coating Technology

The coating part of the research involved the analyses of the raw materials using advanced technologies. From the results of the analyses, the formulation and production of a couple of coatings were carried out. This is followed by the processing and characterization of the produced coatings identified as A, II, III, IV and CG800. Then, benchmarking of the new product (CG800) with other commercial coatings (identified as B, C, D, E, F and G) used for the same application.

The coating was formulated based on the addition of controlled specified amounts of the following constituents: Liquid carrier, refractory filler materials, binder, suspension and dispersing agents, additives like biocides, antifoaming agents, etc. [9] as illustrated in Fig. 2.

In order to determine the presence and source of sulphur, the sand used for making the cores, a filler material (with presumed high S content) used in the coating and the coating were analyzed for sulphur content using LECO chemical analyzer. The sulphur analysis results are shown in Fig. 3. The sulphur (S) content of the cold box sand and the coating are not significantly different from that of the casting. However, the filler showed a relatively high sulphur content but this did not reflect on the amount of S in the coating. This is due to a careful balanced ratio addition relative to the major filler in the coating.

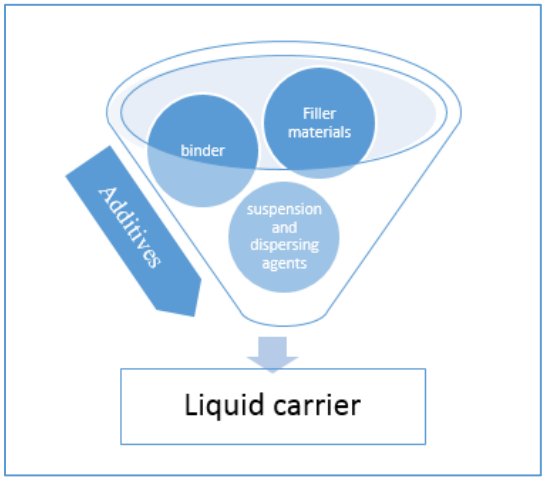

Fig. 2: The coating components [9].

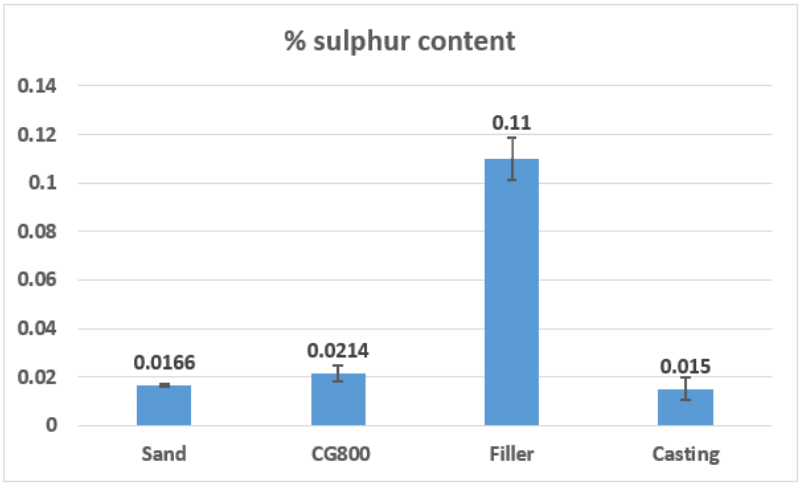

Fig. 3: Sulphur content analysis results from the core sand, ACTICOTE CG800 (CG800), Graphite filler and the casting.

The thermal conductivity of some selected coatings was tested using the Anter Thermal Diffusivity apparatus in Vesuvius Pittsburgh, R&D Centre in the US. The results (Fig. 4) show that Coating A has the lowest thermal conductivity at 1000 °C (considered of interest because it is closer to the melting temperatures) followed by CG800 compared with the other coatings tested. This is expected as Coating A has the coarsest particle size distribution from the particle size distribution (PSD) analysis performed on the coatings (results not shown). A low thermal conductivity (insulation) balanced by other properties such as optimum permeability and high refractoriness (Fig. 4), could be some of the reasons why CG800 performed better than all the other coatings used in the preliminary trials (screening tests).

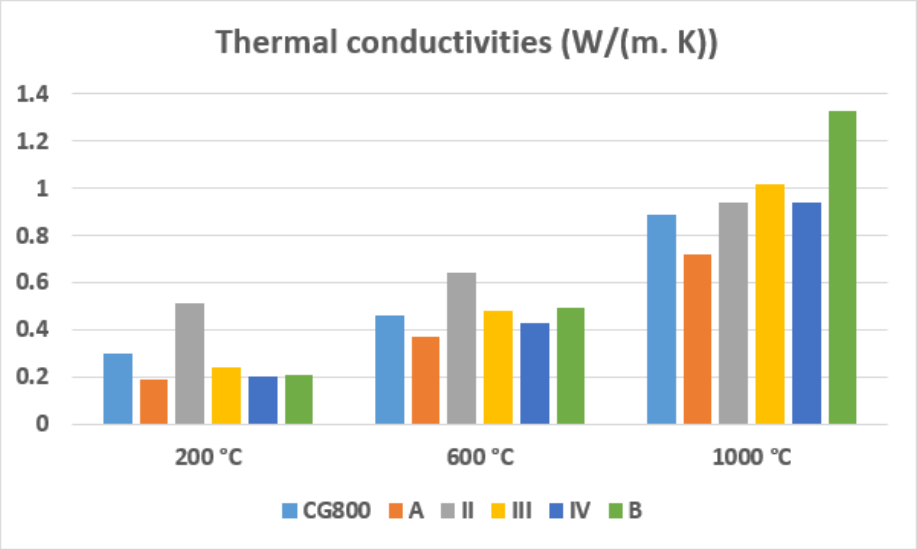

Fig. 4: Thermal conductivities of selected coatings at different temperatures.

The thermal behaviour of CG800, the major filler material used and a modified version of CG800, PID2-20, was analyzed with a heating microscope to determine the characteristic temperatures corresponding to the changes of the shape and the cross-section area of the samples as they are heated. The changes in shape and cross-section of test samples are described by different temperatures namely DT – Deformation temperature (of maximum sintering), ST – Spherical temperature (of initial softening), HT – Hemispherical Temperature (of melting) and FT – Flow Temperature (of flowing) [13]. Further description of these temperatures can be found in ISO 540:2008(E) [14]. The higher these temperatures are, the more refractory the material tested will be. Two other commercial coatings (D and F) were included in the thermal analysis programme. The results are presented in Fig. 5. From the results it can be seen that the pure filler material, vanguard, is more refractory compared with CG800 and PID2-20 and the commercial coatings from their HT temperatures. CG800 has a thermal behaviour similar to that of the filler material, vanguard, from the shaped of the changes occurring on the samples. However, with a slight modification of the filler materials in CG800, by replacing graphite with equal amount of satintone and mica, the thermal behaviour changed significantly, as can be seen in sample shapes of PID2-20. The refractoriness decreased from the DT-deformation temperature up to HT-hemispherical temperature relative to those of CG800. The PID2-20 sample has similar shapes with those of the commercial coatings across all the temperatures. From the transition temperatures, CG800 has comparable refractoriness with the commercial coatings, D and F. The thermal behaviour of CG800 from the transition shapes being different from those of the other coatings could also be one of the reasons for having performance edge over the commercial coatings. This will be investigated further, because the observed transition shapes are not common with heating microscope samples.

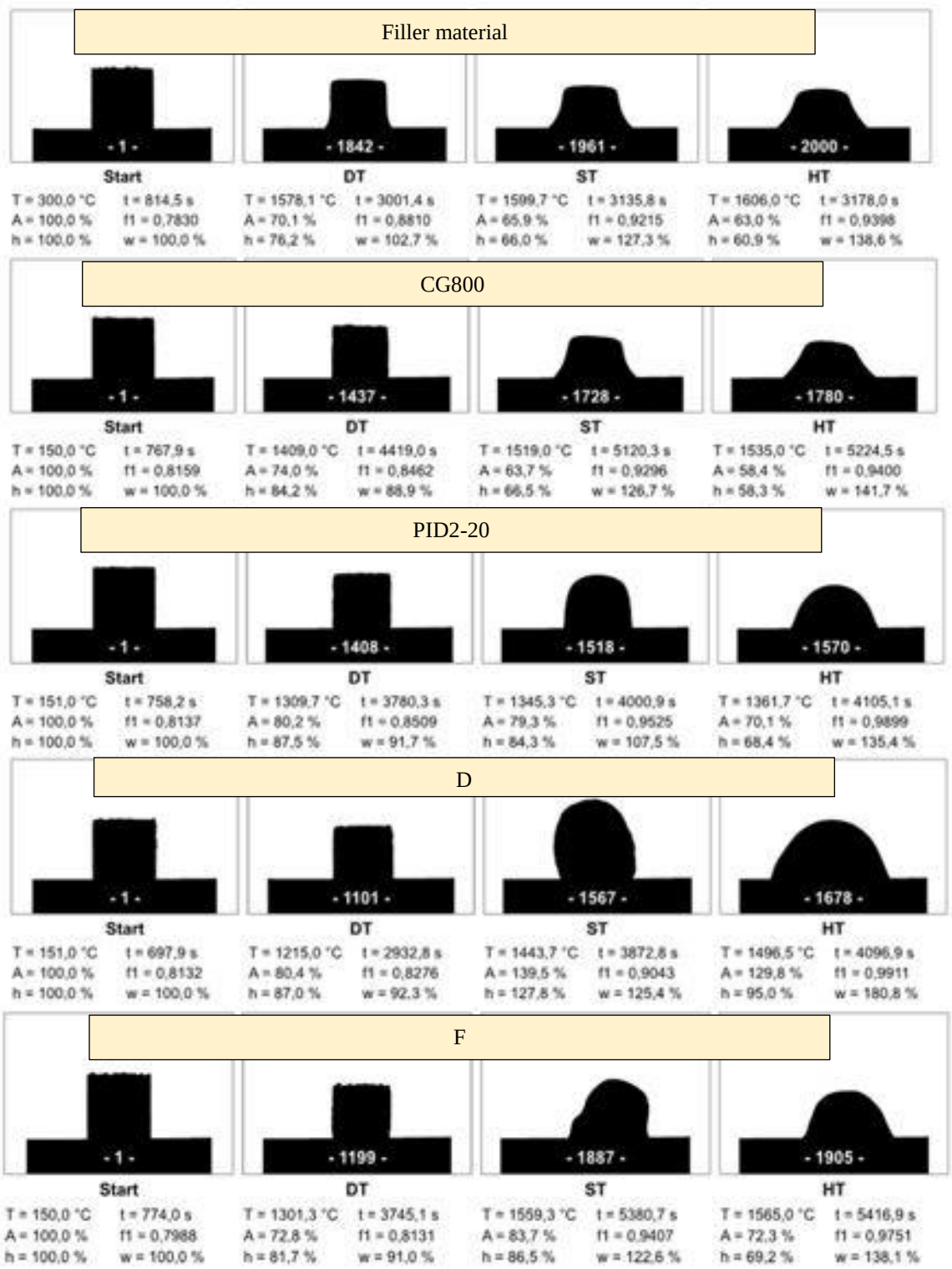

Fig. 5: Heating Microscope images of five samples without thermal expansion properties. Temperatures: Start, DT-deformation temperature, ST-spherical temperature, HT-hemispherical temperature.

The CG800 coating was processed and analyzed alongside some other commercial coatings to determine their foundry application properties. The results obtained (Table 1) showed that the coatings are stable and met the application specifications required by foundries.

Table 1: Foundry coating application properties

Properties	CG800	Other commercial coatings for the same application							Specifications
		A	B	C	D	E	F	G	
Solid content %	63	42.58	42.16	41.88	45.62	44.68	43.27	44.79	40 Minimum
Density gcm^{-3}	1.68	1.37	1.36	1.35	1.4	1.39	1.37	1.38	1.30-1.40
Baume ^{o}Be	108	74	70	58	78	72	60	56	64 Minimum
Diluted coating									
Solid content %	50.62	30.45	32.58	33.2	34.7	32.27	30.86	39.68	
Density gcm^{-3}	1.49	1.24	1.25	1.26	1.28	1.25	1.24	1.33	
Baume ^{o}Be	52	40	38	38	42	42	33	42	28-30
DIN Cup 4 viscosity s	15	14	14	14	16	15	13	15.5	
Matt time s	45 - 50	55					55		
RB number	No flow	12					21		
Adherence	Good	Good	Good	Good	Good	Good	Good	Good	Good
Sedimentation % after 24hrs	1	0.5	0.5	1	1	1	1	1	Stable
Graphite flotation	No	NA	NA	NA	No	No	NA	NA	NA
Dry layer thickness µm	200-230	200-250	200-250	200-250	200-250	200-250	200-320	200-250	230-300

*NA = Not applicable

2.2 Casting Technology

To investigate the behaviour of the different coatings under practical conditions several coating-casting trials were carried out. The casting technology involved the modelling and simulation of the casting process with a commercial software to optimize the geometry for making the tooling. Two simulation results are shown in Fig. 6 showing complete filling and uniform solidification of the hollow cylindrical castings with three different wall thicknesses.

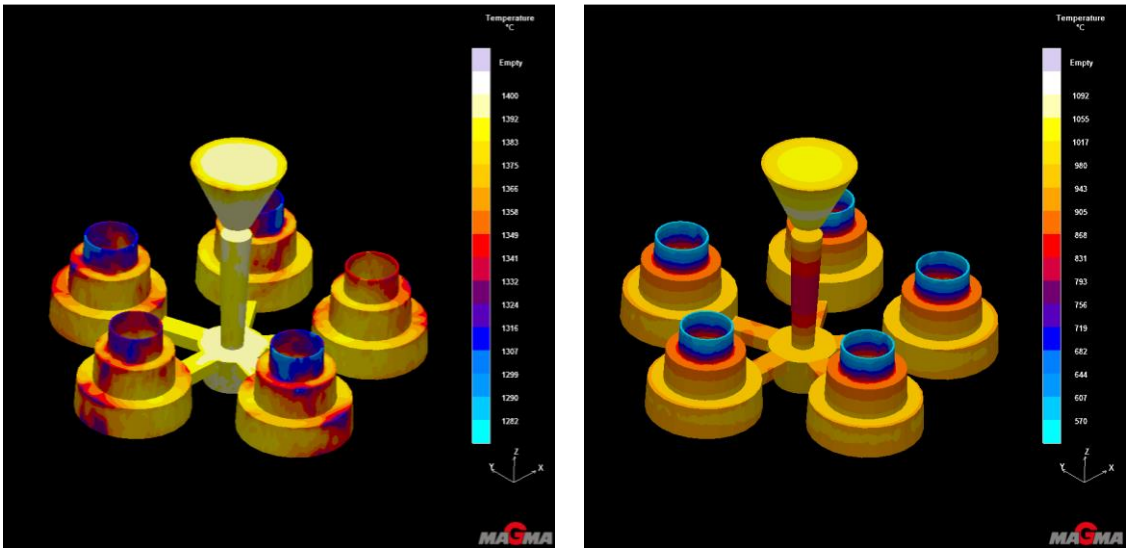

(a) At the end of filling (b) At the end of solidification

Fig. 6: Simulated temperature fields in castings at different times.

Based on satisfactory simulation results, the tooling (Fig. 7) was produced by an external pattern maker. The casting layout shown in Fig. 7, is used to make all the pilot plant trials. This layout ensures that the filling of the casting cavities is done at the same melt temperature, pouring time and melt quality (chemical composition). This layout is robust in that it provides the opportunity to investigate 5 different coating recipes and 3 different casting section thicknesses per casting in one mould. The section thicknesses investigated are 45, 20 and 5 mm identified as X, Y and Z respectively. These different wall thicknesses ensure different contact times between the cores (coatings) and the cast iron melt before it is solidified.

The core is cylindrical in shape with a height of 210 mm out of which 40 mm at the base and 20 mm at the top are core prints with average diameter of 75 mm. The cores are coated by dipping in the coatings which have been diluted and ready for application to achieve a dry layer thickness of around 200 µm. The coated cores are dried in an oven at 120 °C for 2 hours (Fig. 8a). The proud layer thickness of the coating (top layer) and the coating penetrated thickness of the core (penetrated layer) is clearly obvious in Fig. 8b.

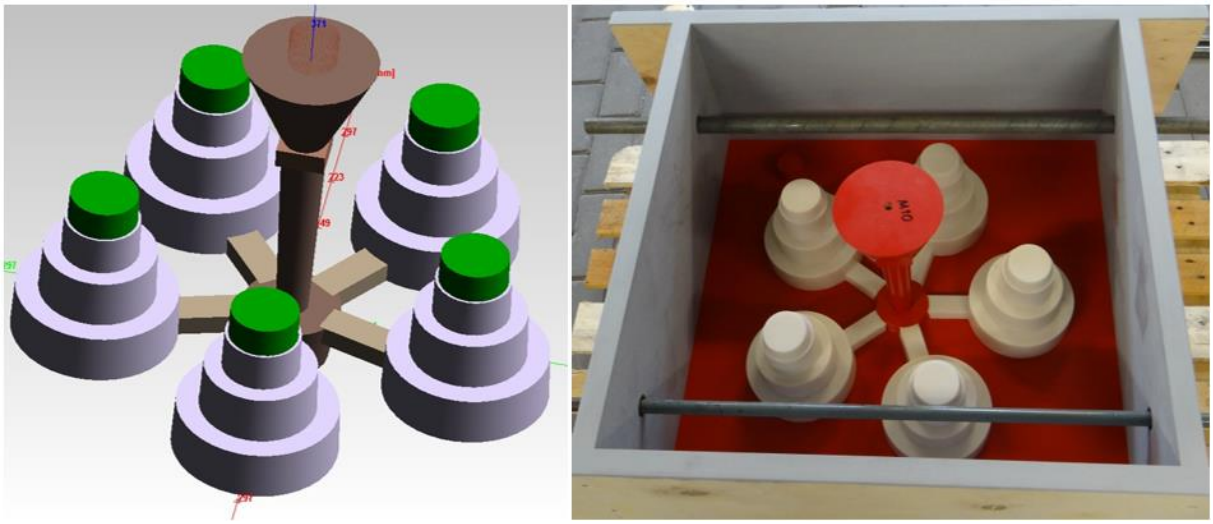

Fig. 7: Casting layout and the tooling used to produce the castings

The casting trials were conducted in a foundry, producing compacted graphite iron castings, according the test programme in Table 3, using SinterCast process. The melt chemical composition is presented in Table 2 and the Sintercast modification index is in the range of 38 – 39 for the various trials. This shows that the melts used for all the trials were consistent in quality and satisfies the calibrated Modification limits, from 38 to 46, required to achieve the microstructure, properties and soundness in the heavy-duty blocks with Sintercast process technology [15].

Table 2: Chemical composition of the melt used for the casting

TC*	Si	Mn	P	S	Cr	Mo	Ni	Cu	Sn	Mg	Fe
3.71	2.36	0.259	0.030	0.019	0.030	0.016	0.039	0.977	0.116	0.013	Bal.

*Total Carbon (TC) – By Thermal Analysis of Base iron, Remainder by spectroscopy of final poured metal.

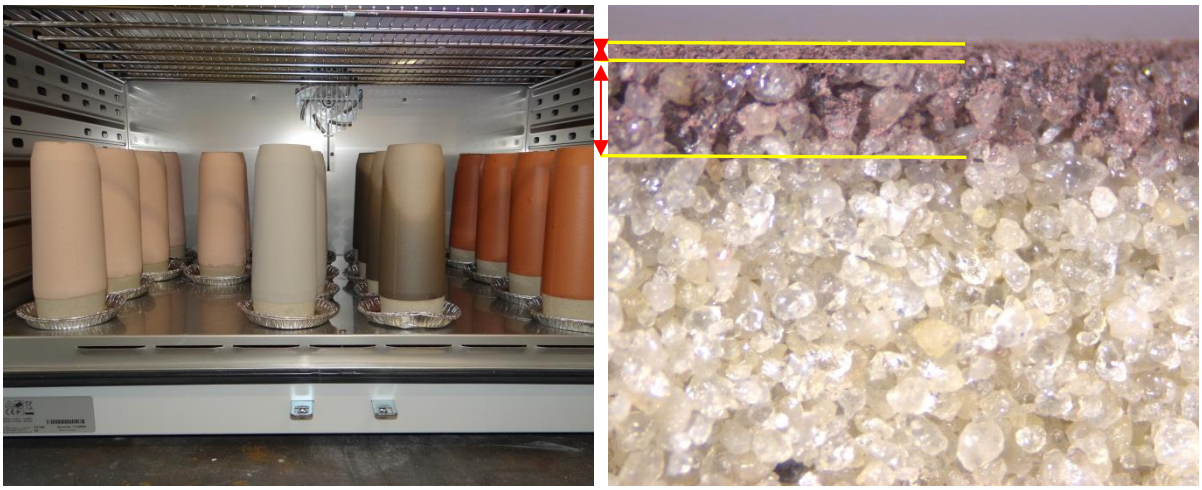

(a) Drying coated cores in an oven (b) Showing top and penetrated layers

Fig. 8: Processing the coated cores

Table 3: Selected casting trials test programme

Test programme		
Trials	Description of trial	Coatings
1	Comparative study of the performance of CG800 with selected coatings, in-house.	A, II, III, IV & CG800
2	Confirmatory performance test (from Trial 1 results)	A & CG800
3	Benchmarking of CG800 with other commercial coatings (external)	CG800, A, B, C, D, E & F
4	Industrial trial with CG800 and some commercial coatings in an external foundry	CG800, A, C & F

3. Results

The results were judged based on the performance of the coatings in reducing the layer of compacted graphite (CG) degeneration to lamellar graphite (LG) at the rim zone of the castings. This performance is evaluated from the microstructures of the castings from various selected trials to compare the performance of ACTICOTE CG800 (CG800) and other commercial coatings used for the same application. The results will be presented according to the content sequence in Table 3. However, the bulk microstructure from selected castings are presented in Fig. 9. It can be seen that the bulk microstructure exhibited typical compacted graphite structure.

From Figs. 10 and 11, it can be seen that the coatings showed different performances on different section thicknesses in the reduction of degenerated CG layer. From the microstructures, it can be said that the layer of degeneration of the CG to FG is section dependent. The defect increases with increasing casting section thickness. This is in agreement with the findings of other researchers and is attributed to the longer solidification and cooling times in the thicker sections [7, 12].

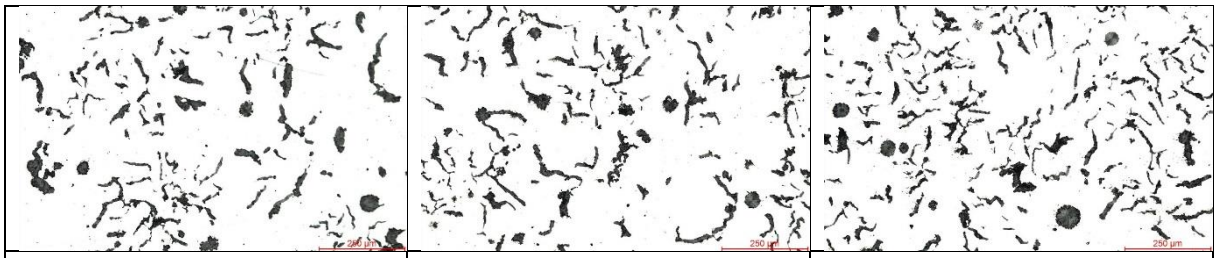

A	III	CG800

Fig. 9: Bulk microstructure from the X-section of three selected castings.

From these figures, it is also clear that the microstructures of the thin section, Z=5 mm, contains uniformly distributed tiny nodules of similar size and distribution. No difference is observed from the effect of the applied coatings. This shows that the solidification of the casting in this thin section was rapid and controlled by the solidification kinetics. There was no time for any diffusion of Sulfur or Oxygen into the melt surface.

Based on the results obtained from the comparative study of the performances of the coatings, Coatings A and CG800 exhibited more positive results relative to the other coatings. Hence, they were subjected to further trial (confirmatory performance test) to ensure the repeatability and reproducibility of their performances. At this stage further investigation of the Z section (5 mm thin section) was dropped, since the coatings have no effect on this section. Further reports of the results will only focus on the 45 and 20 mm section thicknesses.

The results of the confirmatory trial test for Coatings A and CG800 in two replicates each (1 and 2) presented in Fig. 12, show that the performances of the two coatings are consistent in both replicates. Both coatings showed degeneration layer of less than 200 μm. However, CG800 showed a superior performance over Coating A.

ACTICOTE CG800 and Coating A were benchmarked a couple of times with other commercial coatings for the same application, and the results from a selected benchmark trial are presented in Fig. 13. As can be seen, CG800 performed relatively slightly better that the other coatings. However, because the distinction in the performance of CG800 relative to the other coatings in this trial is not very clear, further confirmatory benchmark test was performed. The results from this test is presented in Fig. 14. In Fig. 14, CG800 clearly showed superior performance compared to the other commercial coatings. Based on the results of this trial, it was decided to try ACTICOTE CG800 in a foundry that produces large volumes of CGI engine blocks and cylinder head castings.

ACTICOTE CG800 and three other commercial coatings (A, D and F) were applied on the cores used for the production of water jackets and cylinder heads castings in CGI. After the production of these two products, some samples were collected and investigated on their microstructure evolution at the rim zones. The results on the layer of CG degeneration to FG are presented in Fig. 15. From the figure, it is clear that ACTICOTE CG800 can be applied for the production of CGI castings with significantly reduced CG degenerated layer (less than 150 μm).

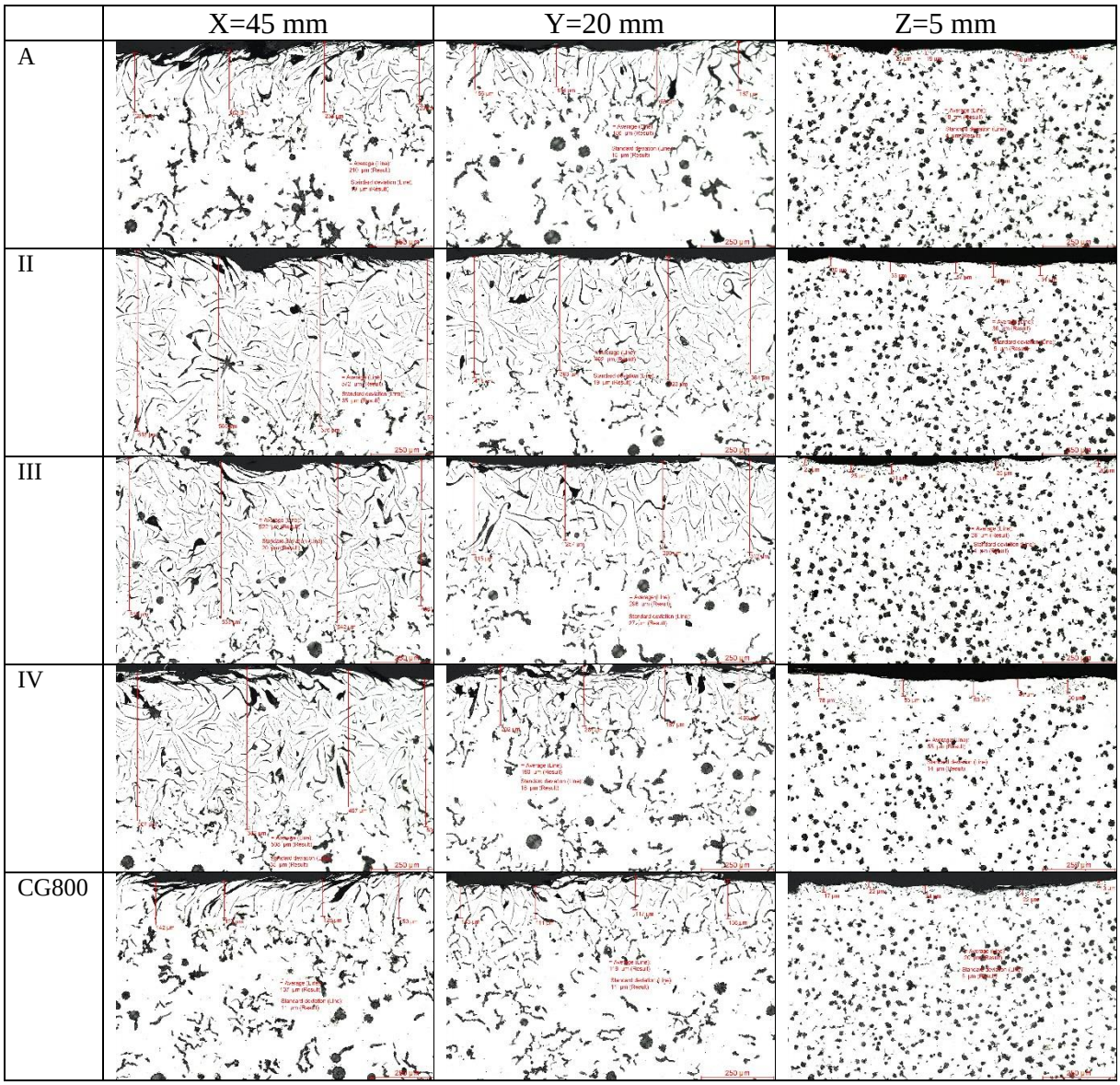

Fig. 10: Interfacial microstructure of the three sections (X, Y & Z) of the castings made with 5 different coatings (A, II, III, IV & CG800) on cores from the comparative study.

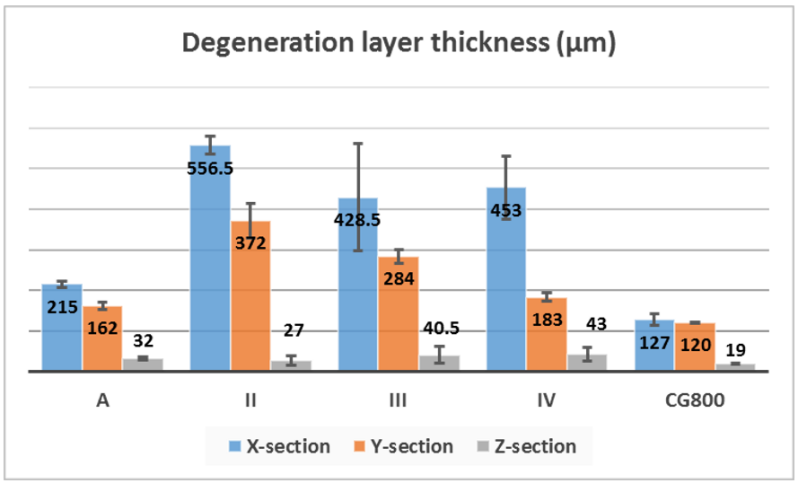

Fig. 11: Effect of the coatings on the layer of degeneration of CG to FG at the surface rim zone of the different section thickness of the castings from the comparative study.

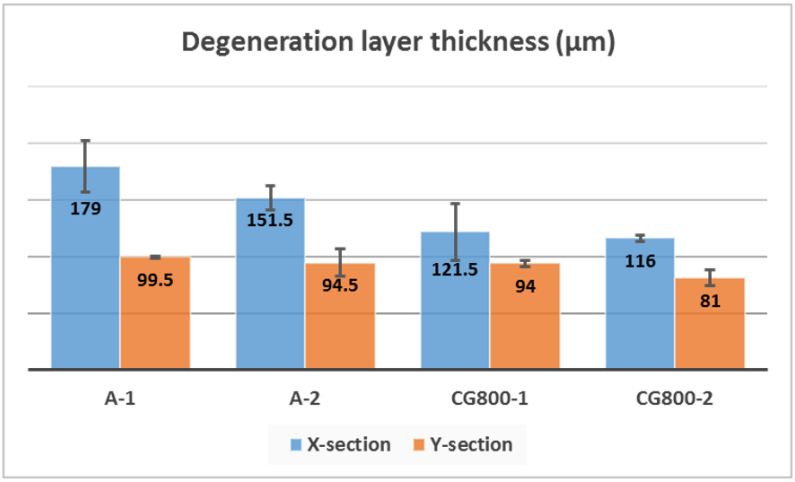

Fig. 12: Effect of the coatings on the layer of degeneration of CG to FG at the surface rim zone of the X and Y sections of the castings from the confirmatory test with Coating A and CG800 in two replicates (1 and 2).

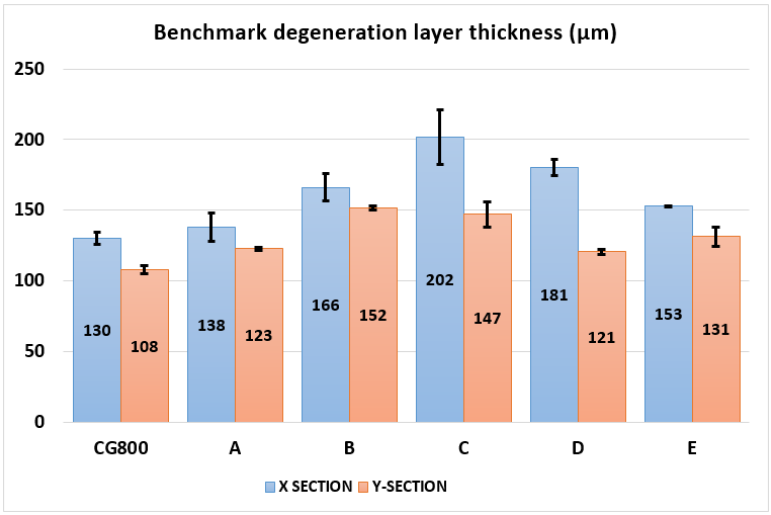

Fig. 13: Effect of CG800 and some selected commercial coatings on the layer of degeneration of CG to FG at the surface rim zone of the X and Y sections of the castings from benchmark trial.

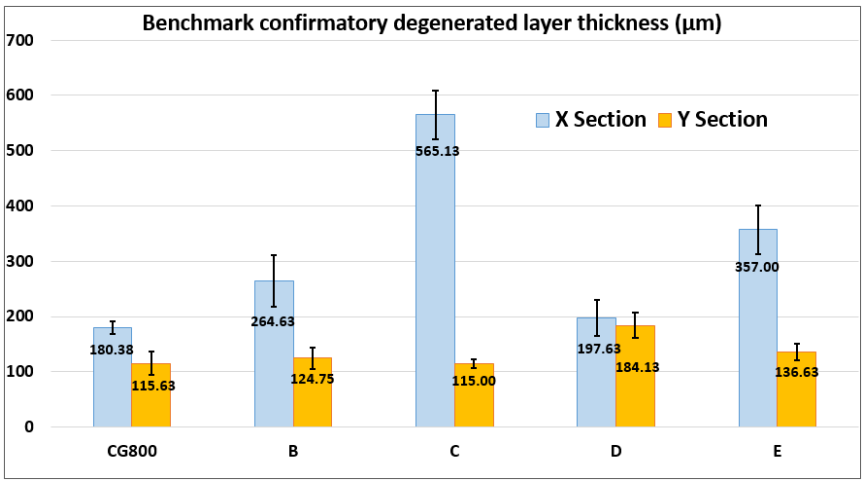

Fig. 14: Effect of the commercial coatings on the layer of degeneration of CG to FG at the surface rim zone of the X and Y sections of the castings from confirmatory benchmark trial.

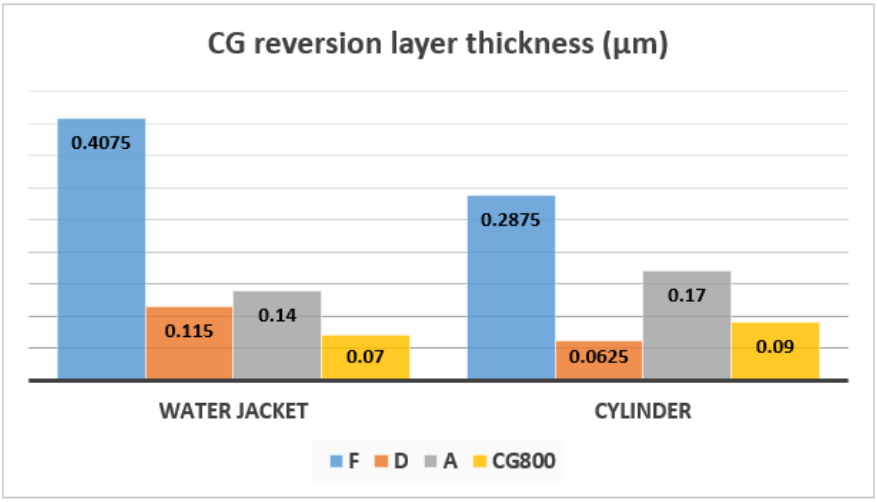

Fig. 15: Effect of the commercial coatings on the layer of degeneration of CG to FG at the surface rim zone of Water jacket and cylinder head castings.

4. Summary

The description of the defect, degeneration of Compacted graphite (CG) to Flake graphite (FG), and the probable causes of this defect have been discussed. The mechanism of defect formation was also mentioned. It was also illustrated that the occurrence and the extent of this defect are dependent on the casting section thicknesses. For remediation, the application of foundry coatings was explored, of which one of them is a new offer from FOSECO, ACTICOTE CG800. The performances of various coatings in reducing the compacted graphite (CG) degeneration layer to flake graphite (FG) and the extent to which this happens have been highlighted. It was extensively shown that ACTICOTE CG800, significantly reduced the occurrence of this defect. This is due to the minimal sulphur content in the coating and insulation properties of the coating coupled with its higher density compared with the other coatings. ACTICOTE CG800 is a water-based coating applied on the cores by dipping method. The coating has stable application properties. The application of the right layer thickness of ACTICOTE CG800 on cores will significantly reduce the degeneration of the compacted graphite at the rim zone of castings of various thicknesses to the barest minimum. This will improve the mechanical properties – tensile and fatigues properties, at the rim zone of castings leading to the reduction of machining allowance and reduction in energy consumption thereby saving cost.

References.

1. **W. Guesser, T. Schroeder and S. Dawson**, Production Experience with Compacted Graphite Iron Automotive Components, AFS Transactions 01-071 (Page 1 of 11).
2. **M. Holtzer, M. Górny and R. Dańko**, Microstructure and Properties of Ductile Iron and Compacted Graphite Iron Castings, The Effects of Mold Sand/Metal Interface Phenomena, Springer 2015.
3. **D.M. Stefanescu, S. Wills and J. Massone**, Quantification of Casting Skin in Ductile and Compacted Graphite Irons and Its Effect on Tensile Properties, AFS Transactions 2009.
4. **I. Riposan, M. Chisamera, S. Stan and T. Skaland**, Surface Graphite Degeneration in Ductile Iron Castings for Resin Molds, ISSN 1007-0214 08/20 Volume 13, Number 2, April 2008 pp157-163.

5. **BCIRA Broadsheet 234** – Flake graphite layers at the cast surfaces of cast nodular iron Castings.
6. **S. Boonmee, D. M. Stefanescu**, Casting Management in Compacted Graphite Iron Part II: Mechanism of Casting Skin Formation, AFS 2013.
7. **International Standard ISO 16112 2006-08-01** – Compacted (vermicular) graphite cast iron – Classification.
8. **U. C. Nwaogu, T. Poulsen, R. K. Stage, C. Bischoff and N. S. Tiedje**, New sol-gel refractory coatings on chemically-bonded sand cores for foundry applications to improve casting surface quality, Surface & Coatings Technology 205 (2011) 4035-4044.
9. **U. C. Nwaogu and N. S. Tiedje**, Foundry Coating Technology: A review, Materials Science and Applications, 2 (2011) 1143-1160.
10. **U. Nwaogu, T. Poulse, B. Gravesen and N. Tiedje**, Using sol-gel component as additive to foundry coatings to improve casting quality, International Journal of cast Metal Research 2012 vol. 25 No.3.
11. **B. Lundeen**, The Influence of Coatings on the Graphite Structure in the Rim Zone of Ductile Iron Castings" DIS Annual Meeting, June 2, 2011, Dallas, Texas.
12. **S. Boonmee, D. M. Stefanescu**, Casting Management in Compacted Graphite Iron Part I: Effect of Mold Coating and Section Thickness, AFS 2013.
13. **W. Panna, P. Wyszomirski and P. Kohut**, Application of hot-stage microscopy to evaluating sample morphology changes on heating, J. Therm. Anal. Calorim. (2016) 125:1053-1059.
14. **International Standard ISO 540:2008(E)** – Hard coal and coke – Determination of ash fusibility.
15. **S. Dawson, P. Popelar**, Thermal Analysis and Process Control for Compacted Graphite Iron and Ductile Iron, SinterCast, Sweden, 2014.